Rare Metal Materials and Engineering
Volume 55, Issue 9, September 2026
Available online at www.rmme.ac.cn

Science Press

Cite this article as: Zhang Langting, Duan Yajuan, Li Bowen, et al. Research Progress on Homogeneous Deformation of Metallic Glasses[J]. Rare Metal Materials and Engineering, 2026, 55(09): 2209-2218. DOI: https://doi.org/10.12442/j.issn.1002-185X.20250552.

REVIEW

Research Progress on Homogeneous Deformation of Metallic Glasses

Zhang Langting[1], Duan Yajuan[2], Li Bowen[2], Qiao Jichao[2]

[1] School of Sciences, Chang'an University, Xi'an 710064, China; [2] School of Mechanics and Transportation Engineering, Northwestern Polytechnical University, Xi'an 710072, China

Abstract: Metallic glasses exhibit exceptional properties but suffer from brittle fracture via shear banding at room temperature. Homogeneous deformation is vital for understanding amorphous plasticity. This review summarized recent advances in homogeneous deformation of metallic glasses in atomic-scale flow mechanisms, evolution of shear transformation zones, flow defects, and hierarchical relaxation processes. The correlation among free volume kinetics, stress-temperature equivalence, and rejuvenation threshold stress was introduced. Role of structural heterogeneity in flow stability was discussed, alongside the application of modern characterization and modeling techniques. The review proposed investigation methods for designing high ductile metallic glasses based on these insights.

Key words: metallic glass; homogeneous deformation; relaxation; shear transformation zone; rejuvenation

1 Introduction

Metallic glasses (MGs), characterized by their disordered atomic structure, represent a distinct class of materials that distinguish them from crystals[1]. This disordered configuration introduces excellent properties, such as superhigh strength and high elastic limit[2–3]. A tendency for localized plastic deformation at shear bands at ambient temperature can be observed, resulting in brittle fracture and negligible macroscopic ductility. To overcome this problem, homogeneous flow has been applied to improve the amorphous plasticity and superplastic forming techniques[4–5]. Although early investigations mainly focus on the high-temperature supercooled liquid region[6–7], recent advances elucidate that the microscopic mechanisms related to homogeneity exist at lower temperatures[8], which are governed by a complex interplay of atomic-scale excitations and a series of relaxation processes[9].

In the past decade, pivotal developments have been made. Deformation mechanisms for hierarchical relaxation processes from fast β'-to-α relaxation have been discussed[10]. The principle of stress-temperature equivalence has been established[11–12], demonstrating that the mechanical energy directly facilitates the structural excitation, which is analogous to thermal energy. A threshold stress for structural rejuvenation has been identified, presenting the boundary between aging-dominated relaxation and net structural disorder that sustains homogeneous flow by promoting shear transformation zone activation[13].

This review summarized the vital advances spanning from atomic-scale mechanisms to macroscopic control of forming processes. The effects of extrinsic factors and intrinsic properties on the stability of homogeneous flow were discussed. The characterization and modeling techniques were presented, as well as the research direction in the future. This review provided a comprehensive insight for the application of the principles to design the strong but ductile MGs with accurate prediction.

2 Physical Perspective: from Hierarchical Excitations to Structural Evolution

Homogeneous flow in MGs originates from their intrinsic structural heterogeneity[14–15]. The physical essence can be

Received date: October 27, 2025
Foundation item: National Natural Science Foundation of China (52271153, 12472069); Natural Science Foundation of Shaanxi Province (2025GH-YBXM-046)
Corresponding author: Qiao Jichao, Ph. D., Professor, School of Mechanics and Transportation Engineering, Northwestern Polytechnical University, Xi'an 710072, P. R. China, E-mail: qjczy@nwpu.edu.cn

conceptualized as follows: under external thermodynamic forces (stress, temperature), a series of localized atomic rearrangements are activated[16–17], and they subsequently evolve and attain long-range spatiotemporal correlations, ultimately manifesting as homogeneous plastic flow. Clarifying this multi-scale dynamic cascade from isolated local excitations to cooperativity is a key to understand the underlying mechanism[18].

The atomic configuration of MGs lies on the potential energy with metastable states[19]. Plastic deformation is enabled by a continuous series of excitations, which can be divided into three parts. (1) β' -relaxation: the localized motions of a few atoms can initiate plasticity[20]. (2) β -relaxation: cooperative rearrangement of tens of atoms can lead to reversible anelasticity[21]. (3) α-relaxation: large atomic clusters can form a percolating network, enabling macroscopic plasticity[22]. This hierarchy represents a continuous sequence from triggering to percolation. Fig. 1a shows the evolution of elastic, anelastic, and viscoplastic strains of this cascade[10].

Macroscopic deformation is governed by internal structural state parameters, particularly the free volume. The stability of homogeneous flow depends on the competition between stress-driven rejuvenation (formation of free volume) and thermally activated aging (annihilation of free volume). A net increase in free volume is essential to maintain the high-energetic state and to prevent strain localization. Fig. 1b – 1c show the relationships between the measured strain of the topological-state MGs and free volume. This approach can calculate the activation volume and energy of flow defects as a function of strain[23]. Fig. 1b shows the strain rate-stress relationship at constant strain with activation volume revealing the growth of cooperating atomic clusters. The Arrhenius plot in Fig. 1c shows the corresponding activation energy, linking the energy to accumulated strain. This strain-based methodology shows that the deformation involves the progressive activation of larger flow units. Fig. 1d synthesizes these concepts, illustrating how the decoupling of thermal and mechanical effects governs the rejuvenation-aging competition and its connection to relaxation dynamics[24].

During homogeneous deformation, small-scale fast process (β') can be transformed to larger-scale slower processes (β and α). Through stress and structural field coupling, discrete shear transition zones (STZs) evolve into spatially correlated zones. When the correlation length approaches the system scale, atomic rearrangements become coordinated, transitioning from localized activations to long-range plastic flow. This universal pattern provides a foundation for understanding and tailoring MG plasticity.

3 Governing Factors and Unified Framework for Homogeneous Flow

At low temperatures (temperature $T \ll$ glass transition temperature T_g), the plasticity is confined to easily activated regions, yielding restricted anelasticity. The critical range for homogeneous flow ($0.7T_g - 0.9T_g$) emerges, when the thermal energy activates cooperative rearrangements[7]. Above T_g, the material behaves as a viscous fluid, deforming homogeneously. Applied stress not only leads to deformation but

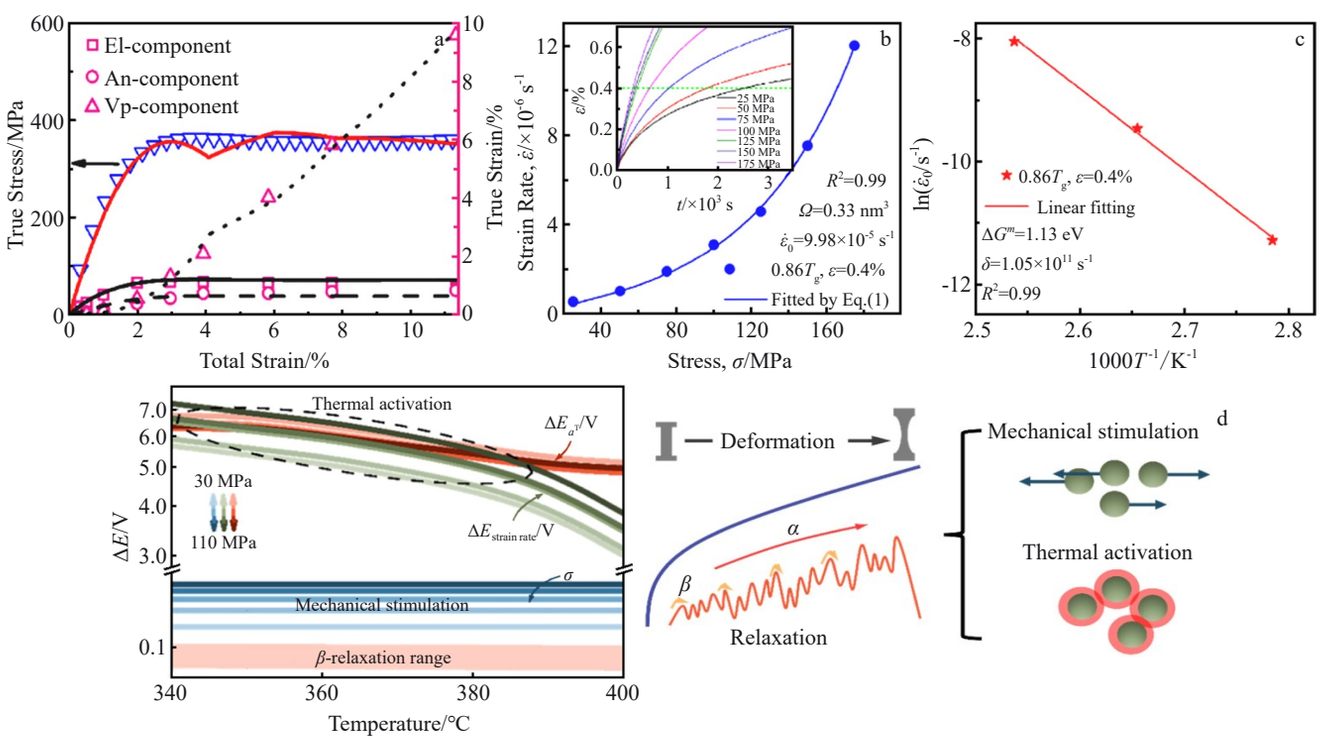

Fig.1 Multi-scale homogeneous flow from physical perspective: (a) evolution of elastic, anelastic, and viscoplastic strains during flow[10]; (b) strain rate as a function of stress at constant strain[23]; (c) Arrhenius plot of strain rate vs. temperature[23]; (d) decoupling thermal and mechanical effects during creep and their correlation with relaxation dynamics[24]

also tailors the energy distribution. Mechanical facilitation lowers activation barriers[25], which is similar to the thermal effect. Higher deviatoric stresses activate larger flow events, extending homogeneous deformation to the region with lower temperatures and higher strain rates[26].

3.1 Critical stress and deformation mode transition

The transition between homogeneous and inhomogeneous flow is governed by a stress threshold with a boundary between aging-dominated relaxation and rejuvenation-driven flow, as illustrated in Fig. 2. Key findings from creep and atomic-scale strain analysis are also shown in Fig.2.

Fig. 2a presents the creep strain evolution under various stresses, revealing a transition in deformation kinetics[27]. At low stress levels, the creep curves exhibit a typical two-stage behavior of primary state and steady state, which is a character of thermally activated diffusion. In contrast, at higher stresses, a tertiary stage emerges, which can be marked by an accelerated strain rate, indicating the onset of mechanical instability. This stress-dependent transition is further quantified in Fig. 2b, where the steady-state creep strain rate follows two distinct power-law scaling regimes separated by a critical stress σ_c[27]. Below σ_c, a linear relationship suggests the Newtonian flow, which is dominated by thermal diffusion. Above σ_c, the power-law exponent $m\approx3$ reflects a non-Newtonian regime, where strain energy gradients drive atomic rearrangements, leading to rejuvenation. The macroscopic stress-strain responses in Fig. 2c – 2d further corroborate this transition[28]. The sample deformed under high stress exhibits significant homogeneous plastic flow before shear banding, as evidenced by the diffusion shear strain contours in the insets of Fig. 2c. In contrast, the sample under low stress shows restricted plasticity and early localization into a shear band, as shown in the insets of Fig.2d.

At the atomic scale, Zhu et al[5] depicted the evolution of local plastic shear strain under small and large strains. Under small strain, plastic deformation is isolated and randomly distributed, reflecting short-range rearrangements driven by thermal energy gradients. Under large strain, however, plastic strain fields become obvious and spatially correlated, indicating long-range cooperative flow enabled by strain energy dominance. These observations align with the abovementioned atomic-scale models[28], confirming that the mechanical stress fundamentally reshapes the energy distribution and changes the relaxation dynamics.

3.2 Intrinsic structural state: competition between rejuvenation and relaxation

The stability of homogeneous flow is governed by the evolution of the structural state parameter during deformation, which is controlled by the competition between rejuvenation and relaxation. This dynamic mode is conceptualized through a deformation-mode map[29], as illustrated in Fig. 3a. The inverse boson peak temperature rises with strain rate for a well-aged MG, signaling a reduction in mechanical stability. This result demonstrates that rejuvenation by lowering the activation barrier for atomic rearrangements, rather than increasing the energy level, directly facilitates the activation of flow defects and stabilizes homogeneous deformation

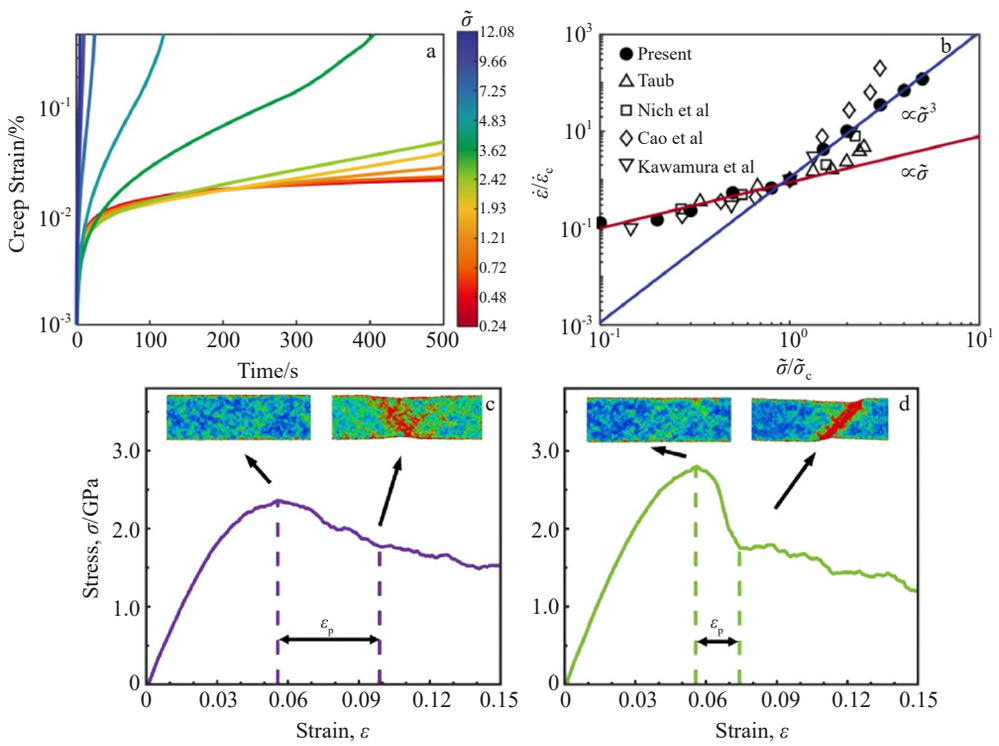

Fig.2 Analysis of transition governed by critical stress from homogeneous flow to inhomogeneous flow: (a) strain evolution under different stresses[27]; (b) scaling of normalized steady-state creep strain rate with normalized stress[27]; (c) macroscopic stress-strain responses under low stress[28]; (d) macroscopic stress-strain responses under high stress[28]

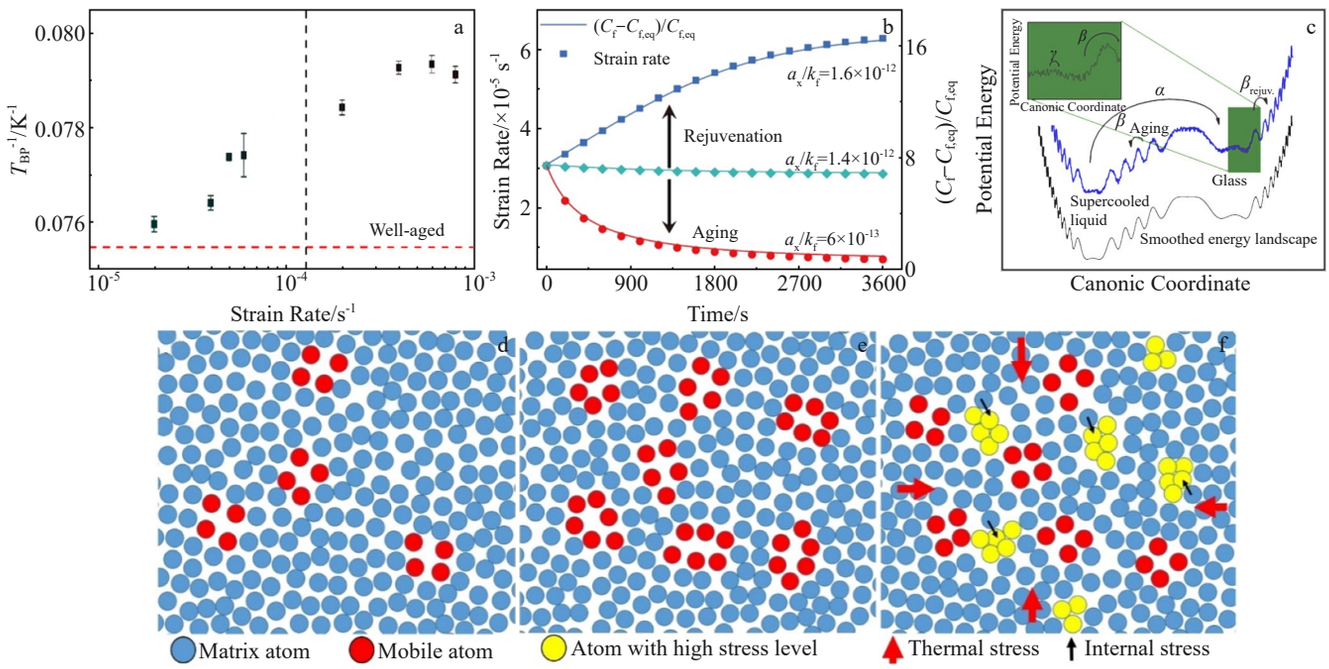

Fig.3 Critical stress and competition between rejuvenation and aging: (a) energetic scales of relevant strain rates[29]; (b) critical stress boundary between rejuvenation state and aging state[30]; (c) energy distribution during transition from aging to rejuvenation[20]; (d) initial state, (e) after-elastostatic-loading state, and (f) after-elastostatic-loading-and-cryogenic-treatment state during microstructure evolution[33]

against localization. As quantified by the free volume model[30], the parameter ratio a_x/k_r, which governs the relative efficiency of formation and annihilation of defects, controls the direction of structural evolution, as shown in Fig. 3b. A lower a_x/k_r ratio leads to a net annihilation of flow defects, while crossing a threshold value induces a global rejuvenation characterized by a net increase in defect concentration[31–32]. This evolution of the relative defect concentration reveals that net structural disordering occurs when the formation rate of defects surpasses the annihilation rate, which is a condition inherently linked to the state with surpassing σ_c.

This critical stress is related to the relaxation hierarchy. Fig.3c represents the energy distribution, highlighting that the stress must be sufficient to activate a series of excitations[20]. The enthalpic peaks in the equivalent configurational heat flow suggest that these processes may involve local bond-breaking of a first-order transition, emphasizing that the stress-driven rejuvenation is not a random disordering process but involves coordinated structural rearrangements related to these relaxation modes. The related microstructure evolution is shown in Fig. 3d – 3f, which demonstrates that elastostatic loading above a critical stress induces atomic expansion and increases the concentration of flow units for both β-relaxation and β'-relaxation, linking mechanical stimulation to enhanced atomic mobility[33]. With the decrease in free volume, subsequent cryogenic treatment generates internal stress and promotes the formation of dense unstable regions with lower activation energy, which triggers plasticity. Therefore, Fig. 3 provides a multi-scale validation, linking the stress threshold and kinetic pathways directly to the underlying atomic-scale structural rearrangements and relaxation dynamics that define the competition between rejuvenation and aging.

In addition, ultrasonic vibration fundamentally alters the flow behavior of MGs by activating their intrinsic dynamic heterogeneity[34]. The high-frequency cyclic loading preferentially activates the fast surface dynamics, drastically reducing the activation energy. This phenomenon leads to an apparent decrease in viscosity by up to several orders of magnitude, accompanied by the expansion of liquid-like regions[35]. As these regions percolate under continuous vibration, they disrupt the surrounding elastic solid-like matrix, inducing a macroscopic fluid-like state[36]. This acoustically-mediated softening effect enables plastic deformation, while maintaining the amorphous structure far below T_g, thus facilitating novel cold joining and forming processes.

3.3 Structural heterogeneity: initial conditions

The chemical composition and the resulting atomic structure establish the baseline potential energy distribution and intrinsic heterogeneity of MGs, thereby presetting their deformation behavior. Fig. 4 shows the effect of initial structural states dictated by composition on the mechanical response across scales of novel high-entropy and conventional MGs.

In high-entropy MGs (Fig. 4a – 4b), the enhanced configurational entropy leads to a distinct structural state characterized by a high degree of short-range order and denser atomic packing[37]. This results in superior hardness and elastic modulus compared to their low- and medium-entropy counterparts, which is attributed to the sluggish dynamics effect. The pronounced nanoindentation creep displacement observed at high loading rates signals a high susceptibility to activate flow defects under high strain rates.

In conventional MGs (Fig. 4c – 4f), compositional tuning

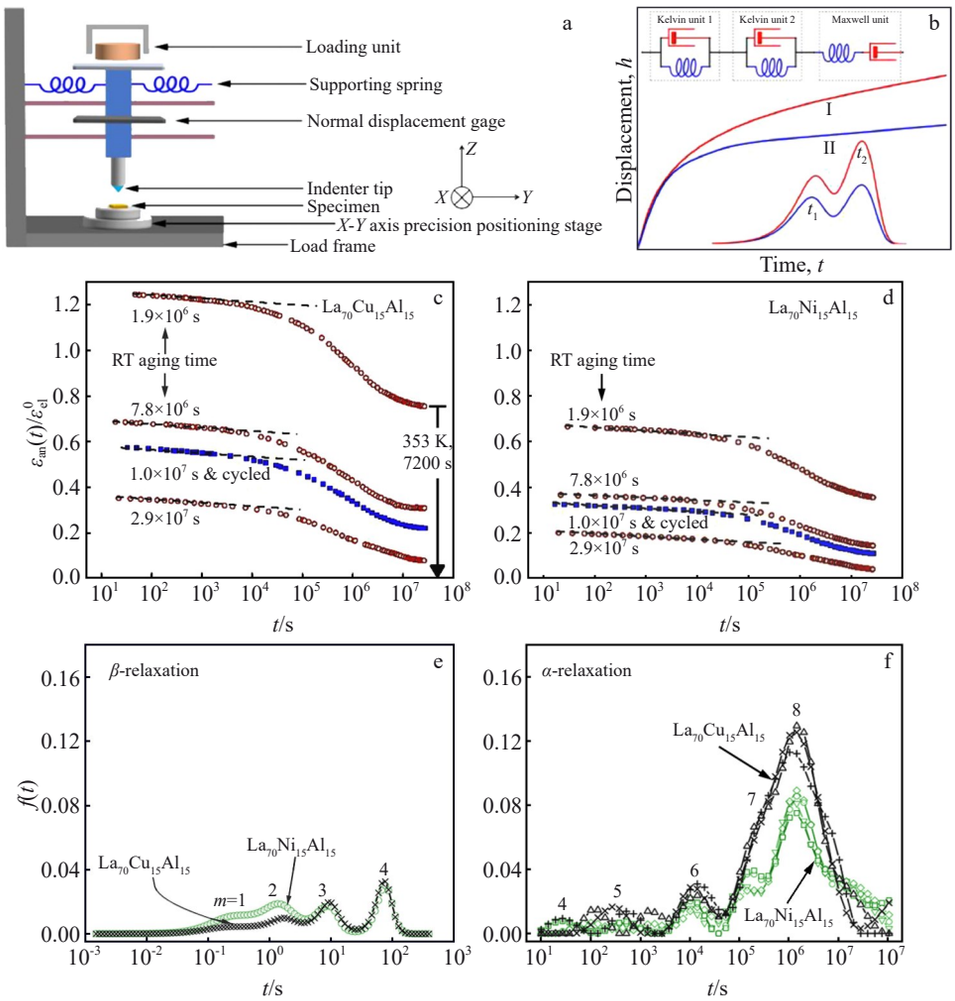

Fig.4 Effects of initial chemical composition and structural state on mechanical response across scales of novel high-entropy and conventional MGs: (a) schematic diagram of measurement instrument[37]; (b) schematic diagram of creep displacement curves[37]; (c) normalized anelastic strain rejuvenation for $La_{70}Cu_{15}Al_{15}$ with different relaxation behavior[31]; (d) normalized anelastic strain rejuvenation for $La_{70}Ni_{15}Al_{15}$ with different relaxation behavior[31]; (e) relaxation-time curves with m=1–4 derived from bending measurements[38]; (f) relaxation-time curves with m=4–8 derived from bending measurements[38]

(e.g., comparison between $La_{70}Cu_{15}Al_{15}$ and $La_{70}Ni_{15}Al_{15}$) directly alters the hierarchy of STZs[31,38]. Quasi-static anelastic relaxation measurements reveal that a pronounced β-relaxation is linked to a higher fraction of small fast potential STZs and a lower fraction of large slow STZs. However, tensile tests show that superior plasticity correlates with a higher density of STZs[39], particularly in the α-relaxation region, which sustains a more homogeneous activation[40].

The initial structure state can be represented by the population and distribution of flow defects or STZs, which serve as the primary governor. Whether modulated by high-entropy effects or conventional composition design, a structure with a sufficient activatable flow units, especially those enabling long-range correlation, promotes the stability of homogeneous flow. Fig.4 shows the critical roles of initial chemical composition and structural heterogeneity, and it emphasizes that the initial structural state quantified via STZ distributions can predict the deformation mode transitions and change MG composition for enhanced ductility and formability.

3.4 Synthesized perspective: deformation-mode phase diagram

The effects of external stress and intrinsic structural state, resulting in the competition between rejuvenation and aging, can be synthesized into a deformation-mode map. Fig. 5 provides a multi-scale validation, linking macroscopic mechanical response directly to the underlying atomic-scale relaxation dynamics and structural evolution.

The fundamental principle enabling this framework is the stress-temperature equivalence, as shown in Fig. 5a. The temperature-stress-transformation diagram[41], derived from molecular dynamics (MD)-dynamic mechanical spectroscopy simulations, reveals that a static load can effectively lower T_g. This finding confirms that mechanical energy can facilitate the large-scale cooperative atomic rearrangements, which are the characteristics of the α-relaxation, thereby expanding the thermodynamic window for homogeneous flow. Fig.5b further

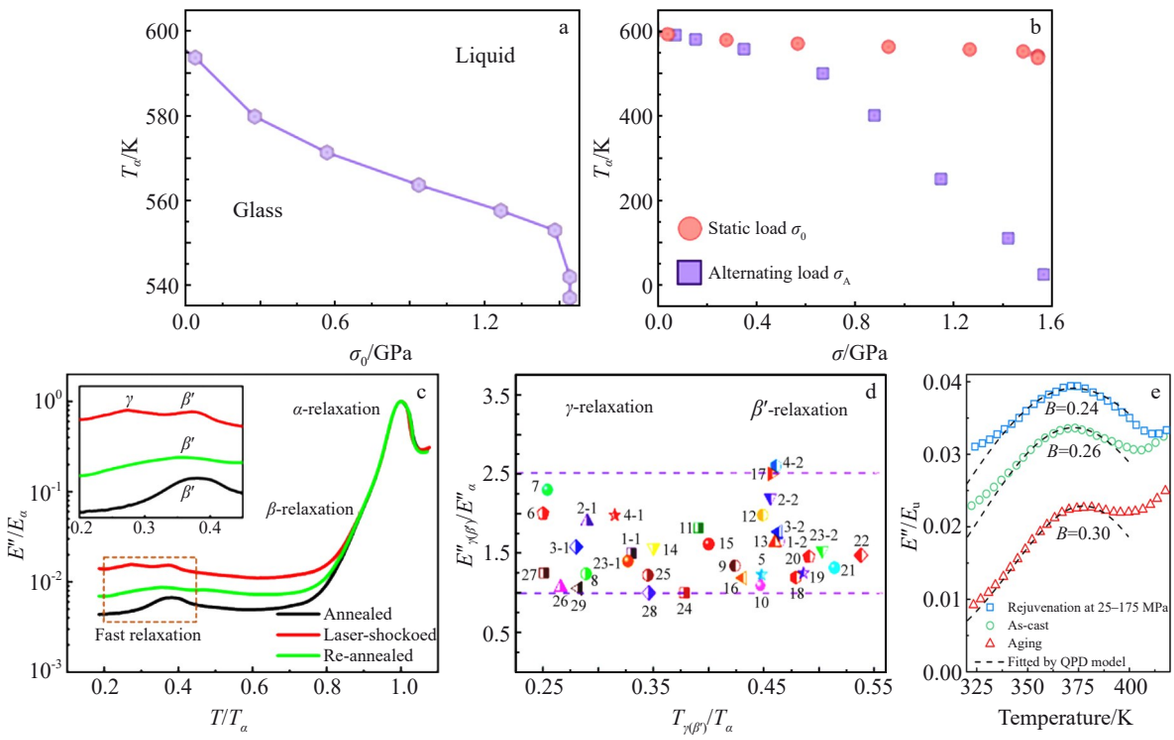

1-1, 1-2: $Dy_{55}Co_{20}Al_{25}$; 2-1, 2-2: $Dy_{55}Co_{20}Al_{25}Si_1$; 3-1, 3-2: $Dy_{55}Co_{20}Al_{25}Si_3$; 4-1, 4-2: $Dy_{18}Er_{18}Y_{18}Ni_{26}Al_{20}$; 5: $La_{56.16}Ce_{14.04}Ni_{19.8}Al_{10}$; 6: $Zr_{58.5}Cu_{15.6}Ni_{12.8}Al_{10.3}Nb_{2.8}$; 7: $Zr_{66.5}Cu_{33.5}$; 8: $Pd_{77.5}Cu_6Si_{16.5}$; 9: $La_{55}Co_{20}Si_{25}$; 10: $Y_{55}Co_{20}Al_{25}$; 11: $Nd_{55}Co_{20}Al_{25}$; 12: $Sm_{55}Co_{20}Al_{25}$; 13: $Gd_{55}Co_{20}Al_{25}$; 14: $Tb_{55}Co_{20}Al_{25}$; 15: $Ho_{55}Co_{20}Al_{25}$; 16: $Er_{55}Co_{20}Al_{25}$; 17: $Tm_{55}Co_{20}Al_{25}$; 18: $La_{60}Ni_{15}Al_{25}$; 19: $La_{58.5}Ni_{16.5}Al_{25}$; 20: $Ce_{54}Cu_{21}Al_{25}$; 21: $Ce_{63.36}Co_{24.62}Al_{10}Fe_2$; 22: $Ce_{61.2}Cu_{23.8}Al_{10}Fe_5$; 23-1, 23-2: $Pd_{40}Cu_{30}Ni_{20}P_{10}$; 24: $Zr_{41.2}Ti_{13.8}Cu_{12.5}Ni_5Be_{22.5}$; 25: $Zr_{46.8}Ti_{8.2}Cu_{7.5}Ni_{10}Be_{27.5}$; 26: $Zr_{52.5}Ti_5Cu_{17.9}Ni_{14.6}Al_{10}$; 27: $Zr_{55}Cu_{30}Ni_5Al_{10}$; 28: $Zr_{35}Cu_{8.25}Ti_{30}Be_{26.75}$; 29: $Cu_{46}Zr_{46}Al_8$

Fig.5 Stress-induced reshaping of energy distribution and relaxation: (a) temperature-stress-transformation diagram[41]; (b) T_g reduction induced by alternating load[41]; (c) splitting of β'-relaxation peak into γ and β' peaks after laser-shock loading[42]; (d) universal scaling of fast secondary relaxation intensities vs. normalized temperature for MGs[43]; (e) enhancement of slow β-relaxation intensity in recovered MG[44]

contrasts this effect with that of alternating load[41], which induces a more dramatic reduction in T_g due to the additional activation of flow units by strain rate effects and the promotion of atomic rearrangement overlap. This direct comparison emphasizes that the specific mode of mechanical loading, whether static or dynamic loading, changes the energy distribution and the kinetics of glass transition. This result is represented by a framework for understanding homogeneous deformation under diverse thermomechanical conditions.

Crucially, the influence of mechanical stimulation is not confined to the α -relaxation but extends to the entire relaxation hierarchy. Fig. 5c offers a typical example[42], showing how laser-shock loading can split a single fast β'-relaxation peak into two distinct peaks: a γ-relaxation at lower temperatures and a β'-relaxation at higher temperatures. The γ -relaxation is linked to the excitation of less stable medium-range orders. The universal nature of these fast processes[43–45] is further highlighted in Fig. 5d, which summarizes data from various MGs and shows a clear boundary between the γ and β' regions around $0.4T_\alpha$. This universal scaling shows that the fast relaxation is an intrinsic process of the dynamic heterogeneity in MGs.

The consequence of activating these relaxation processes is a net shift in the energetic state. This is quantitatively captured in Fig. 5e, which depicts the evolution of the normalized loss modulus for MG in recovered, as-cast, and aged states[44]. The application of mechanical cycling (rejuvenation) significantly enhances the intensity of the slow β-relaxation and broadens its distribution. This enhancement signals an increase in the population and mobility of flow defects, which directly changes to a higher propensity for homogeneous plastic flow by facilitating the nucleation and percolation of shear transformations[46].

In summary, Fig. 5 collectively elucidates that the mechanical stress simultaneously facilitates the primary α-relaxation and reconstructs the secondary relaxation by reshaping the potential energy distribution. This multi-scale excitation from the triggering of fast γ -relaxation and β' -relaxation to the eventual cooperation in the α-relaxation alters the balance in the continuous competition between rejuvenation and aging.

4 Probing and Modeling Spatiotemporal Evolution of Deformation

Synergistically integrating current experiments and multi-scale modeling is necessary. Techniques, such as dynamic mechanical analysis, particularly under a superimposed static stress, have been pivotal in establishment of the stress-temperature equivalence. The systematic stress-induced shift of the α-relaxation peak provides direct experiment evidence that mechanical energy directly facilitates large-scale

cooperative motions, which is a foundational principle for homogeneous flow. The evolution of β -relaxation with thermal and mechanical history correlates with the population and mobility of flow defects. Furthermore, the non-exponential relaxation described by the Kohlrausch-Williams-Watts (KWW) function[47–49] is far more than a fitting tool. The stretched exponent β_{KWW} is a quantitative metric for the dynamic heterogeneity. Its correlation with the change rate of free volume creates a crucial bridge, inferring microscopic structural kinetics from macroscopic mechanical or calorimetric data. Fig. 6 provides the origin of β_{KWW}[50]. This modified diffusive-trapping model considers that the applied strain fundamentally reshapes the potential energy distribution. It allows atomic excitations to diffuse and become trapped in this reconfigured distribution. The change rate of free volume governs this process: a slow change rate (the structure evolution is minimal) favors compressed exponential relaxation (β_{KWW}>1), which is the characteristic of internal stress redistribution or caged atomic hopping. Conversely, a fast change rate of free volume driven by mechanical stimulation promotes this band-mediated diffusive trapping, leading to the stretched exponential decay (β_{KWW}<1), which is the characteristic of heterogeneous dynamics during rejuvenation and flow.

MD simulations offer atomic-scale deformation processes, which can identify the fundamental operation of STZs, visualizing the nucleation and percolation of shear bands, and validating scaling laws[39,51]. MD can directly observe the string-like collective rearrangements of β-relaxation and even the faster β' processes, providing a relation between atomic structure and mechanical response. The vital challenge is to establish a direct causal relation between the fundamental relaxation processes and the macroscopic mechanical performance of MGs. While the individual roles of α-relaxation and β-relaxation processes have been extensively studied, their interplay and corresponding mechanism governed by the energetic state have remained complex, particularly in the deep supercooled liquid region where crystallization cannot be presented by conventional experiments. Fig.7 shows advanced nano-calorimetry and MD to resolve this problem, providing a unified multi-scale framework.

Fig.7a shows the critical coupling degree separating regions where β -relaxation is pronounced or appears as an excess wing[52]. Fig. 7a–7b show a universal critical coupling degree $1-n$ that dictates the relaxation mode in the supercooled liquid[52]. This critical value validated across metallic, polymeric, and oxide glasses separates two distinct regions[52]. (1) Low coupling region ($1-n$<0.47): the β -relaxation is pronounced and decoupled early from the α-relaxation process upon cooling (β separated from α). This early decoupling preserves a high population of flow units in the glassy state. (2) High coupling region ($1-n$>0.47): the β -relaxation can only be observed as an excess wing, and the α -relaxation process can be observed from a continuous β -relaxation process upon cooling (α separated from β), resulting in fewer more-isolated flow units. The mechanical implication is that the glasses in the low-coupling region exhibit superior plasticity. The atomic-scale origin of this behavior can be revealed by MD simulations. Fig. 7c shows the fraction of atomic rearrangements in MGs under strain, revealing the atomic-scale origin of homogeneous flow. It can be seen that the systems with a pronounced β-relaxation and low $1-n$ value exhibit a high fraction of atomic rearrangements (string-like cooperativity)[53]. This is a direct atomic-level signature of the interconnected flow units that promote the homogeneous plasticity. In contrast, systems with weak β -relaxation show more randomized displacements, leading to localized deformation. This phenomenon is further verified by mesoscale modeling, which incorporates the activation energy. The model quantifies the effect of initial energetic state on the average activation barrier and softening potential. It is suggested that the lower the initial energy, the larger the required average activation energy, which promotes strain localization despite increasing the yield strength[54]. These results are summarized in Fig.7d–7e.

Collectively, the initial energetic state (set by composition and processing) dictates the α - β coupling degree, which

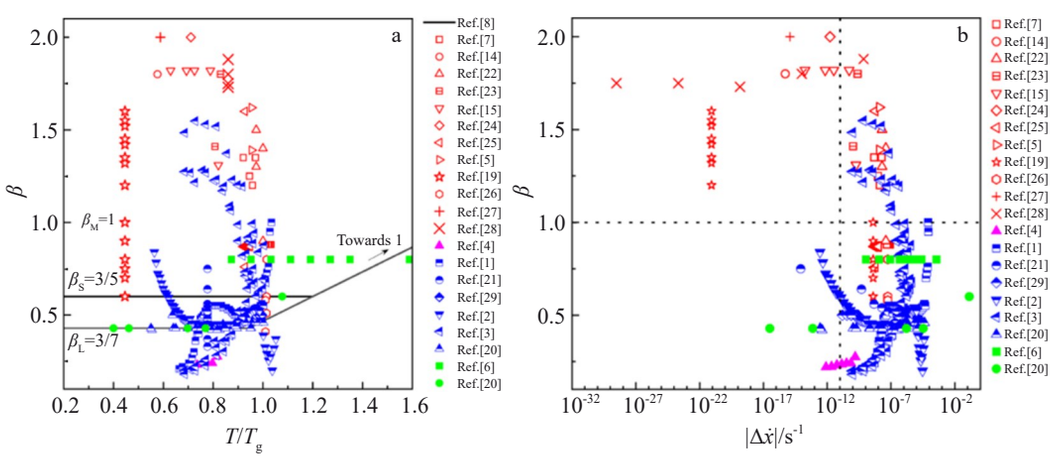

Fig.6 Relationship between relaxation kinetics and atomic-scale free volume dynamics[50]: (a) relationship between KWW stretching exponent β and homologous temperature of various MGs; (b) stretching exponent as a function of change rate of free volume

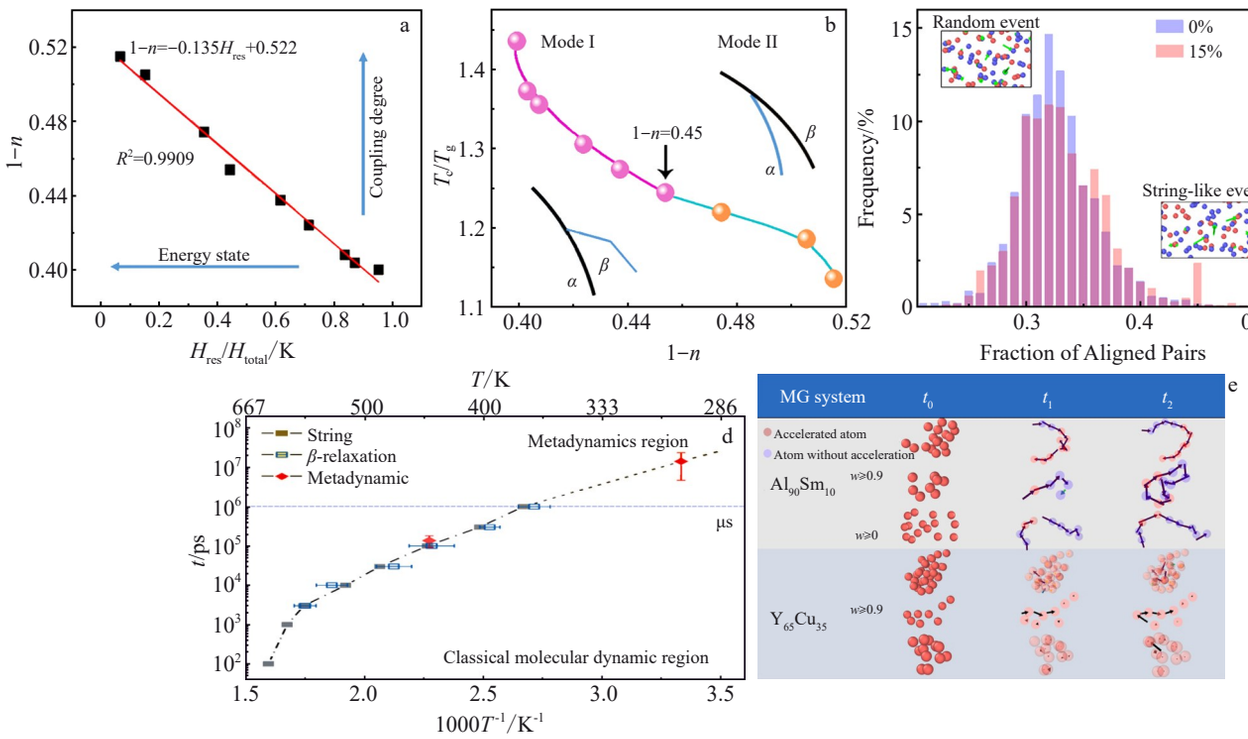

Fig.7 Multi-scale relationship between α-β relaxation coupling and plasticity: (a) critical coupling degree[52]; (b) relationship between critical temperature ratio and coupling degree[52]; (c) fraction of atomic rearrangements in MGs under strain[53]; (d) β-relaxation map of $Al_{90}Sm_{10}$ MG[54]; (e) schematic diagram of cooperative rearrangements of accelerated atoms and their surroundings in $Al_{90}Sm_{10}$ and $Y_{65}Cu_{35}$ MGs[54]

microscopically leads to the propensity for string-like rearrangements. This atomic-scale cooperativity governs the stability of homogeneous flow at the mesoscale and ultimately determines the macroscopic ductility. This multi-scale understanding provides a quantitative analysis for designing MGs with designed mechanical properties by controlling their relaxation hierarchy through thermal and mechanical history[55–57].

5 Summary and Outlook

Despite significant achievements, several fundamental challenges remain in achieving a predictive understanding and control of homogeneous flow in MGs. Addressing the following problems requires a concerted shift from phenomenological description to predictive science and controlled engineering.

1) The initial stages of plasticity: the occurrence mechanism of plastic deformation from the initial atomic scale to the formation of a stable shear transformation is still obscure. A primary challenge is the direct and quantitative experiment for investigation of the fast relaxation dynamics (β') and their causal relationship with the nucleation of flow defects. Prevailing techniques often lack the combined temporal resolution and sensitivity to probe these fast events. The development of ultrafast high-resolution mechanical tests and the application of low-temperature X-ray photon spectroscopy are promising methods to capture the dynamics. Coupled with atomic simulations designed to isolate these triggers, a concerted effort is needed to establish a complete distribution map of plasticity from the initial β' trigger, through the β-relaxation, to the eventual α-scale cooperation.

2) Towards predictive modeling across time and space: current constitutive models incorporating the key physics often fall short in predicting long-term performance and behavior under complex loading. Two critical gaps exist. One is predicting deformation over decades, which requires models to integrate the continuous competition between physical aging and mechanical rejuvenation. Current accelerated testing protocols need to be validated against these coupled kinetics. The other one is that most models are calibrated for uniaxial or simple shear loading. The behavior under multi-axial, non-proportional, or cyclic loading, where the directions of stress and strain rate are different, is profoundly complex and can barely be captured. Next-generation models must incorporate tensorial state variables and anisotropic damage evolution.

3) The ultimate challenge lies in linking fundamental knowledge to materials and manufacturing processes. The proven efficacy of protocols, such as elastostatic loading and cryogenic cycling, must be systematized. A fundamental understanding should be investigated on the following perspectives: how these treatments activate the relaxation processes, and how much the rejuvenation threshold stress is needed for different MGs and component geometries. Additionally, the comprehensive Ashby-type map for MGs is still rare, which can reliably predict the transition among homogeneous flow, shear banding, and fracture as a function

of stress, temperature, strain rate, and the initial structural state. Integrating the rejuvenation threshold stress as a central boundary is a critical milestone.

References

1 Zhou Z Y, Yang Q, Yu H B. *Progress in Materials Science*[J], 2024, 145: 101311

2 Riechers B, Das A, Rashidi R *et al*. *Materials Today*[J], 2025, 82: 92

3 Li F, Zhang Z, Liu H *et al*. *Nature Materials*[J], 2024, 23: 52

4 Zhang L T, Duan Y J, Wang Y J *et al*. *Acta Mechanica Sinica*[J], 2026, 40(8): 425311

5 Zhu W Q, Deng Y J, Liu J J *et al*. *Modelling and Simulation in Materials Science and Engineering*[J], 2024, 32(3): 035026

6 Nieh T G, Wadsworth J. *Scripta Materialia*[J], 2006, 54: 387

7 Schuh C A, Lund A C, Nieh T G. *Acta Materialia*[J], 2004, 52(20): 5879

8 Nabahat M, Amini N, Pineda E *et al*. *Physical Review Materials*[J], 2022, 6: 125601

9 Costa M B, Londoño J J, Blatter A *et al*. *Acta Materialia*[J], 2023, 244: 118551

10 Hao Q, Lyu G J, Pineda E *et al*. *International Journal of Plasticity*[J], 2022, 154: 103288

11 Song S, Zhu F, Chen M. *Nature Materials*[J], 2022, 21: 404

12 Guan P, Chen M, Egami T. *Physical Review Letters*[J], 2010, 104: 205701

13 Ding G, Jiang F, Song X *et al*. *Science China: Physics, Mechanics & Astronomy*[J], 2022, 65: 264613

14 Hong Y R, Wang H, Li X *et al*. *Matter*[J], 2023, 6(4): 1160

15 Im S, Wang Y C, Zhao P Y *et al*. *Physical Review Materials*[J], 2021, 5: 115604

16 Gao T H, Rüßmann P, Wang Q W *et al*. *Nature Physics*[J], 2023, 19: 1896

17 Chang C, Zhang H P, Zhao R *et al*. *Nature Materials*[J], 2022, 21: 1240

18 Pica C M, Ji W, Wyart M. *Proceedings of the Indian National Science Academy*[J], 2024, 121: e2400611121

19 Zella L, Moon J, Egami T. *Nature Communications*[J], 2024, 15: 1358

20 Spieckermann F, Şopu D, Soprunyuk V *et al*. *Nature Communications*[J], 2022, 13: 127

21 Yu H B, Wang W H, Bai H Y *et al*. *National Science Review*[J], 2014, 1: 429

22 Hao Q, Xing G, Pineda E *et al*. *Science China: Physics, Mechanics & Astronomy*[J], 2024, 68: 234611

23 Zhang L T, Wang Y J, Nabahat M *et al*. *International Journal of Plasticity*[J], 2024, 174: 103923

24 Liang S Y, Zhang L T, Wang B *et al*. *International Journal of Mechanical Sciences*[J], 2025, 302: 110573

25 Yuan C C, Lv Z W, Li X *et al*. *Intermetallics*[J], 2023, 153: 107803

26 Zhang L, Duan Y, Crespo D *et al*. *Science China: Physics, Mechanics & Astronomy*[J], 2021, 64: 296111

27 Zhu W Q, Liu J J, Mao S *et al*. *Journal of the Mechanics and Physics of Solids*[J], 2021, 146: 104216

28 Song J Q, Zhu W Q, Wei X D. *International Journal of Mechanical Sciences*[J], 2021, 204: 106570

29 Gao Y, Ding G, Yang C *et al*. *Journal of Non-Crystalline Solids*[J], 2023, 615: 122410

30 Zhang L T, Wang Y J, Yang Y *et al*. *Science China: Physics, Mechanics & Astronomy*[J], 2022, 65: 106111

31 Lei T J, DaCosta L R, Liu M *et al*. *Acta Materialia*[J], 2019, 164: 165

32 Ross P, Küchemann S, Derlet P M *et al*. *Acta Materialia*[J], 2017, 138: 111

33 Balal A H, Bian X L, Han D X *et al*. *International Journal of Plasticity*[J], 2025, 189: 104356

34 Li X, Li L Y, Sohrabi S *et al*. *Science Bulletin*[J], 2024, 69(2): 163

35 Ma J, Yang C, Liu X D *et al*. *Science Advances*[J], 2019, 5(11): eaax7256

36 Li L Y, Li X, Huang Z Y *et al*. *Nature Communications*[J], 2023, 14: 6305

37 Li W, Zuo X F, Liu R *et al*. *International Journal of Plasticity*[J], 2024, 174: 103893

38 Lei T J, DaCosta L R, Liu M *et al*. *Acta Materialia*[J], 2020, 195: 81

39 Urata S, Li S. *Acta Materialia*[J], 2018, 155: 153

40 Lu H M, Zhang Z H, Tang Y *et al*. *Journal of the Mechanics and Physics of Solids*[J], 2024, 192: 105806

41 Sun H J, Chang C, Zhou H B *et al*. *Physical Review B*[J], 2025, 111: 184107

42 Yang C, Duan J, Ding G *et al*. *Physical Review B*[J], 2024, 109: 024201

43 Shao L, Xue L, Qiao J *et al*. *Scripta Materialia*[J], 2023, 222: 115017

44 Zhang L T, Wang Y J, Pineda E *et al*. *International Journal of Plasticity*[J], 2022, 157: 103402

45 Küchemann S, Maaß R. *Scripta Materialia*[J], 2017, 137: 5

46 Gan K F, Jiang S S, Huang Y J *et al*. *International Journal of Plasticity*[J], 2019, 119: 1

47 Atzmon M. *Journal of Applied Physics*[J], 2018, 123: 065103

48 Zhang L T, Wang Y J, Yang Y *et al*. *International Journal of Mechanical Sciences*[J], 2024, 281: 109661

49 Tong Y, Song L, Gao Y *et al*. *Nature Communications*[J], 2023, 14: 8407

50 Chen Y, Sun Y H, Wang W H. *Physical Review B*[J], 2024, 110: 134309

51 Şopu D. *Journal of Alloys and Compounds*[J], 2023, 960: 170585

52 Ding Y J, Shi F L, Wang X P *et al*. *Acta Materialia*[J], 2024, 266: 119698

53 Wang Y C, Wang Y C, Liu C Y *et al*. *Acta Materialia*[J], 2024,

276: 120136

54 Zhou Z Y, Sun Y, Gao L *et al*. *Acta Materialia*[J], 2023, 246: 118701

55 Guan H, Kou H C, Wang J *et al*. *Rare Metal Materials and Engineering*[J], 2014, 43(5): 1047

56 Ma Z H, Dong X H, Su H J *et al*. *Rare Metal Materials and Engineering*[J], 2012, 41(10): 1706

57 Zong H T, Ma M Z, Li L X *et al*. *Rare Metal Materials and Engineering*[J], 2013, 42(3): 470

金属玻璃均匀变形研究进展

张浪渟[1]，段亚娟[2]，李博文[2]，乔吉超[2]

(1. 长安大学 理学院，陕西 西安 710064)

(2. 西北工业大学 力学与交通运载工程学院，陕西 西安 710072)

摘　要：金属玻璃性能优异，但在室温以剪切带形式脆性断裂。均匀变形对于理解金属玻璃的塑性至关重要。本文综述了近年来金属玻璃均匀变形行为的研究进展，重点从原子尺度流动机制、剪切转变区演化、结构缺陷与多层次弛豫行为等方面展开讨论，并介绍了自由体积动力学、应力-温度等效性及无序化临界应力等关键概念。讨论了结构非均匀性对流动稳定性的影响，评述了现代表征与模拟技术的应用，并在此基础上展望了设计高塑性金属玻璃的研究路径。

关键词：金属玻璃；均匀变形；弛豫；剪切转变区；无序化

作者简介：张浪渟，男，1998年生，博士，副教授，长安大学理学院，陕西 西安 710064，E-mail：langtingzhang@chd.edu.cn